Human Molecular Genetics, 2018, Vol. 27, No. 18 3129–3136

doi: 10.1093/hmg/ddy216
Advance Access Publication Date: 5 June 2018
Original Article

ORIGINAL ARTICLE

Impaired melanocortin pathway function in Prader–Willi syndrome gene-*Magel2* deficient mice

Merve Oncul†, Pelin Dilsiz†, Edanur Ates Oz, Tayfun Ates, Iltan Aklan, Esref Celik, Nilufer Sayar Atasoy and Deniz Atasoy*

Department of Physiology, School of Medicine, Regenerative and Restorative Medical Research Center (REMER), Istanbul Medipol University, Istanbul 34810, Turkey

*To whom correspondence should be addressed at: Department of Physiology, School of Medicine, Istanbul Medipol University, Istanbul 34810, Turkey. Tel: +90 44485445437; Fax: +90 2125317555; Email: datasoy@medipol.edu.tr

Downloaded from https://academic.oup.com/hmg/article-abstract/27/18/3129/5033383 by guest on 08 January 2020

Abstract

Prader–Willi Syndrome (PWS) is a neurodevelopmental disorder causing social and learning deficits, impaired satiety and severe childhood obesity. Genetic underpinning of PWS involves deletion of a chromosomal region with several genes, including *MAGEL2*, which is abundantly expressed in the hypothalamus. Of appetite regulating hypothalamic cell types, both AGRP and POMC-expressing neurons contain *Magel2* transcripts but the functional impact of its deletion on these cells has not been fully characterized. Here, we investigated these key neurons in *Magel2*-null mice in terms of the activity levels at different energy states as well as their behavioral function. Using cell type specific *ex vivo* electrophysiological recordings and *in vivo* chemogenetic activation approaches we evaluated impact of *Magel2* deletion on AGRP and POMC-neuron induced changes in appetite. Our results suggest that POMC neuron activity profile as well as its communication with downstream targets is significantly compromised, while AGRP neuron function with respect to short term feeding is relatively unaffected in *Magel2* deficiency.

Introduction

Prader–Willi Syndrome (PWS) is a complex neuro-developmental disorder characterized by insatiable appetite, childhood obesity, social and learning deficits (1–4). Genetic defects underlying PWS involve paternal loss of the 15q11-q13 region that contains the protein coding genes *MKRN3, MAGEL2, NDN, NPAP1* and *SNURF-SNRPN*. Among these proteins, MAGEL2 is highly and almost exclusively expressed in the hypothalamus, suggesting that its absence may contribute to impaired energy homeostasis (5–7). In addition to its deletion in PWS, truncating point mutations of paternal *MAGEL2* allele cause Schaaf–Yang syndrome, which has overlapping phenotype with PWS (7,8).

Mice with *Magel2* gene deficiency display increased weight gain and adiposity accompanied with high leptin levels (9). Within the hypothalamus, *Magel2* is densely expressed in the arcuate nucleus (ARC) (10,11), which harbors distinct neuronal populations that antagonistically regulate appetite and energy expenditure (12). Both, orexigenic AGRP-expressing neurons and anorexigenic POMC-expressing neurons have been reported to contain *Magel2* transcripts (13). Recent studies showed that in *Magel2* deficient mice, POMC neurons have impaired leptin response that may be caused by reduced LepR trafficking to the cell surface (14–16). Furthermore, *Magel2* knock-out mice appear to be hypersensitive to MC4R activation and display reduced POMC-neuron axon arborization phenotype (10,14,15,17).

These studies suggest that altered leptin sensitivity in POMC neurons may contribute to impaired energy balance; however, whether similar disruptions take place for AGRP neurons have not been investigated. More importantly, it is not known how the lack of *Magel2* affects behavioral function of POMC neurons.

†These authors contributed equally to this work.
Received: May 10, 2018. **Revised:** May 29, 2018. **Accepted:** May 30, 2018

© The Author(s) 2018. Published by Oxford University Press. All rights reserved.
For permissions, please email: journals.permissions@oup.com

In the present study, we used a combination of *ex vivo* electrophysiology and chemogenetic behavioral analysis to characterize the activity levels of both AGRP and POMC neurons in *Magel2* null background and examined whether these neurons can still engage with downstream circuits to positively or negatively influence food intake, respectively. Our results suggest that while voracious feeding phenotype of AGRP neuron activation remains unaffected, POMC neuron activity patterns as well as its satiety-inducing function are significantly impaired.

Results

Loss of *Magel2* alters baseline firing properties of POMC but not AGRP neurons

Dysfunction in hypothalamic feeding circuits may underlie increased adiposity and late onset weight gain seen in *Magel2* deficient mice. To investigate how baseline activities of AGRP and POMC neurons from *Magel2* null mice compare with those seen in wild-type littermates, we used florescence guided loose-seal recordings from acute brain slices in which neuronal internal milieu is kept relatively intact. To achieve this, we labeled AGRP neurons in 6–7 weeks old *Agrp-cre* or *Agrp-cre::Magel2*$^{+m/-p}$ double transgenic mice using Cre-recombinase-dependent Green Fluorescent Protein (GFP) expressing virus, *rAAV2/8-FLEX-GFP* and waited for 10–14 days for transgene expression (Fig. 1A and B). Under *ad libitum* feeding conditions, baseline firing rates of AGRP neurons were similar in *Agrp-cre* or *Agrp-cre::Magel2*$^{+m/-p}$ mice as measured from acute brain sections (Fig. 1C and E). Previous reports have shown defective compensatory refeeding response following food deprivation in *Magel2* null mice (14), which may be caused from insufficient AGRP neuron activation upon starvation. We therefore measured whether AGRP neuron activity can properly adapt to food

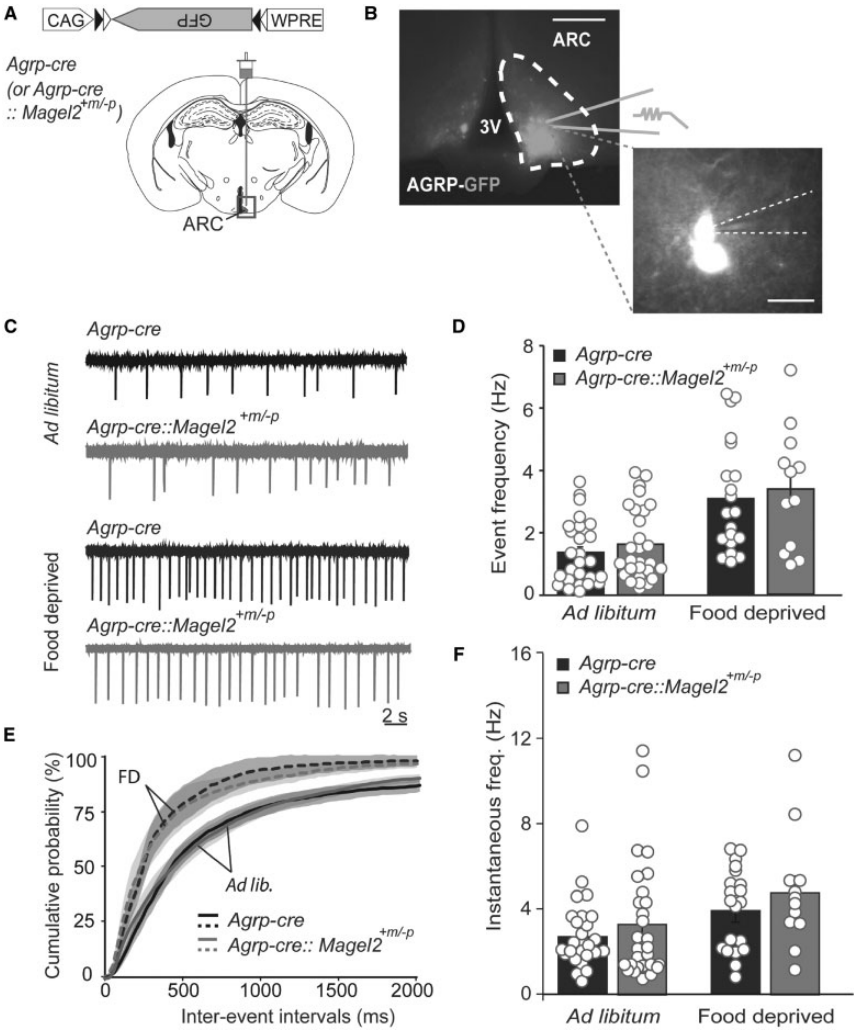

Figure 1. AGRP neuron activity levels are not affected in *Magel2*-deficient mice. (**A**) Schematic drawing for Cre-dependent rAAV expression of GFP in AGRP neurons. (**B**) Photomicrograph of GFP labeled AGRP neurons in arcuate nucleus. (Scale: 300 μm, 20 μm; ARC: arcuate nucleus; 3V: 3rd ventricle). (**C**) Representative traces of loose seal recordings showing action currents from AGRP neurons of *Agrp-cre* and *Agrp-cre::Magel2*$^{+m/-p}$ mice. (**D**) Frequency graph for spontaneous activity of AGRP neurons in both sated (*Agrp-cre*: 1.32 ± 0.20 Hz, $n = 26$ neurons from five mice and *Agrp-cre::Magel2*$^{+m/-p}$: 1.59 ± 0.21 Hz, $n = 28$ neurons from three mice; $P = 0.37$) and food deprived (*Agrp-cre*: 3.07 ± 0.40 Hz, $n = 20$ neurons from three mice and *Agrp-cre::Magel2*$^{+m/-p}$: 3.37 ± 0.56 Hz, $n = 12$ neurons from two mice; $P = 0.66$) conditions. (**E**) Cumulative probability of inter-event interval plot for spontaneous activity of AGRP neurons from *Agrp-cre* and *Agrp-cre::Magel2*$^{+m/-p}$ mice in sated and food deprived conditions. Shaded areas represent SEM. (**F**) Summary graph for instantaneous firing rates of AGRP neurons from *Agrp-cre* and *Agrp-cre::Magel2*$^{+m/-p}$ mice in sated (Agrp-cre: 2.71 ± 0.30 Hz, $n = 26$ neurons from five mice and *Agrp-cre::Magel2*$^{+m/-p}$: 3.30 ± 0.52 Hz, $n = 28$ neurons from three mice; $P = 0.34$) and food deprived (Agrp-cre: 3.93 ± 0.42 Hz, $n = 20$ neurons from three mice and *Agrp-cre::Magel2*$^{+m/-p}$: 4.75 ± 0.78 Hz, $n = 12$ neurons from two mice; $P = 0.33$) conditions.

Downloaded from https://academic.oup.com/hmg/article-abstract/27/18/3129/5033383 by guest on 08 January 2020

deprivation in *Magel2* null mice. As expected, food deprivation significantly increased activity levels in *Agrp-cre* mice, which was not significantly different from AGRP neuron firing rate measured from 24-h food deprived *Agrp-cre::Magel2*$^{+m/-p}$ mice (Fig. 1C and E). Instantaneous firing rates were comparable in all groups (Fig. 1F).

Deficits in leptin receptor function have been cited in POMC neurons with *Magel2* deletion (14–16) but how this defect influences baseline POMC neuron activity has not been described. We hypothesized that leptin insensitivity in these mice may result in reduced baseline activity levels in POMC neurons. To test this, we compared POMC neuron firing rates under fed state, which was significantly lower in *Pomc-cre::Magel2*$^{+m/-p}$ mice compared with *Pomc-cre* littermates (recorded from 8 to 9 weeks old mice, Fig. 2A and E). Interestingly, a closer examination of firing patterns revealed that, POMC neurons from *Magel2* null mice had significantly lower instantaneous firing rates (Fig. 2F). Collectively, these results suggest that *Magel2* gene product is required for normal POMC neuron firing pattern, while it is dismissible for the baseline activity levels of AGRP neurons and their ability to respond to negative energy balance.

Impact of AGRP or POMC neuron activation on food consumption in *Magel2* deficient mice

Downstream effectors of ARC^{AGRP} and ARC^{POMC} neurons are the key elements in energy balance regulation. It is not clear whether these neurons can still effectively mobilize downstream circuits to fulfill their behavioral function in *Magel2* deficient mice. Therefore, we next explored the behavioral consequences of selective activation of AGRP and POMC neurons, specifically focusing on free feeding phenotype. We initially addressed whether orexigenic features of AGRP neurons were maintained in the absence of *Magel2* gene. We first tested the impact of an orexigenic hormone, ghrelin that is known to influence feeding, at least in part, through AGRP neurons (18). Intraperitoneal injection of ghrelin (0.5 mg/kg) on light cycle increased food intake in both wild-type and mutant mice similarly (>Supplementary Material, Fig. S1). This result suggests that the orexigenic machinery responsible for ghrelin dependent feeding effect is still intact in *Magel2* null mice. To further characterize capacity of AGRP-neuron dependent orexigenic phenotype, we used chemogenetic DREADD

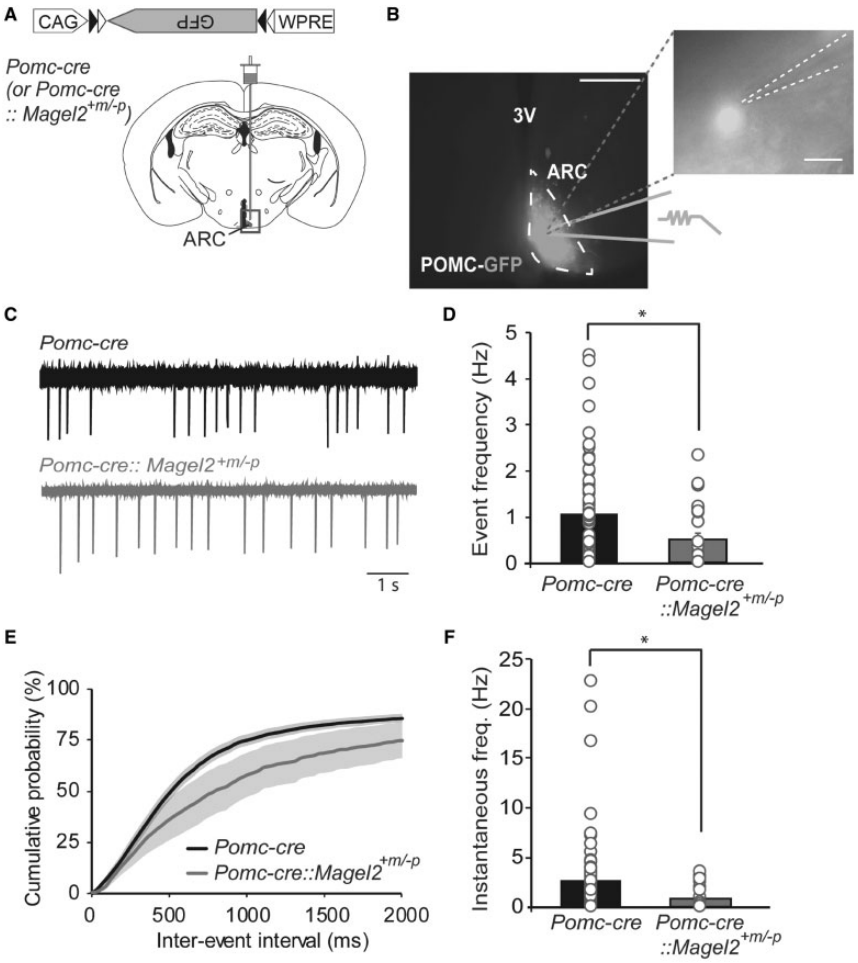

Figure 2. POMC neuron activity is altered in *Magel2*-deficient mice. (**A**) Schematic drawing for Cre-dependent rAAV expression of GFP in POMC neurons. (**B**) Photomicrograph of GFP labeled POMC neurons in arcuate nucleus. Scale: 300 μm, 20 μm; ARC, arcuate nucleus; 3V, 3rd ventricle. (**C**) Representative traces of *ex vivo* loose seal recordings of action currents from POMC neurons of *Pomc-cre* and *Pomc-cre::Magel2*$^{+m/-p}$ mice. (**D**) Frequency graph for spontaneous activity of POMC neurons in sated condition (*Pomc-cre*: 1.03 ± 0.11 Hz, $n = 82$ neurons from four mice and *Pomc-cre::Magel2*$^{+m/-p}$: 0.48 ± 0.13 Hz, $n = 25$ neurons from three mice; $P = 0.01$). (**E**) Cumulative probability of inter-event interval plot for spontaneous activity of POMC neurons from *Pomc-cre* and *Pomc-cre::Magel2*$^{+m/-p}$ mice in sated conditions. Shaded areas represent SEM. (**F**) Summary graph for instantaneous firing rates of POMC neurons from *Pomc-cre* and *Pomc-cre::Magel2*$^{+m/-p}$ mice (*Pomc-cre*: 2.60 ± 0.42 Hz, $n = 82$ neurons from four mice and *Pomc-cre::Magel2*$^{+m/-p}$: 0.83 ± 0.24 Hz, $n = 25$ neurons from three mice; $P < 0.02$) (*$P < 0.05$).

Downloaded from https://academic.oup.com/hmg/article-abstract/27/18/3129/5033383 by guest on 08 January 2020

technology to directly and selectively activate AGRP neurons. We transduced AGRP neurons with Cre-dependent *rAAV2/1-EF1a-DIO-hM3D(Gq)-mCherry* virus in *Agrp-cre* or littermate *Agrp-cre::Magel2*$^{+m/-p}$ mice (Fig. 3A and B). We stimulated AGRP-hM3D neurons by intraperitoneal injection of the DREADD ligand clozapine N-oxide (CNO) and recorded short-term food intake in 8–10 weeks old male subjects. Acute activation of AGRP neurons provoked robust increase in food consumption in both *Agrp-cre* or *Agrp-cre::Magel2*$^{+m/-p}$ mice (Fig. 3C and D). Body weights of both groups were not significantly different from each other (Fig. 3E). Thus, AGRP neurons can efficiently promote food intake even in the absence of functional *Magel2* gene.

Unlike AGRP neurons, POMC neurons in the ARC do not affect short-term food intake but can effectively suppress it over 24-h period upon chronic stimulation (19,20). We next explored the impact of prolonged POMC neuron activation on food intake using chemogenetics. Following transduction of POMC neurons in *Pomc-cre* and *Pomc-cre::Magel2*$^{+m/-p}$ mice with *rAAV2/1-EF1a-DIO-hM3D(Gq)-mCherry* virus (Fig. 4A and C), we monitored food intake for 15 days through daily CNO injections between Days 5 and 10 and saline on other days. Upon CNO delivery, average food intake was significantly suppressed in both *Pomc-cre* and *Pomc-cre::Magel2*$^{+m/-p}$ mice (Fig. 4D and E; 8–10 weeks old male subjects). However, the extent of appetite suppression was much weaker in *Pomc-cre::Magel2*$^{+m/-p}$ mice compared with *Pomc-cre* littermates (Fig. 4F). There were no significant changes in body weights during saline and CNO treatments in both groups (Fig. 4G). Collectively, these results suggest that even full activation of POMC neurons in *Magel2* null mice fails to effectively reduce long-term food intake.

Discussion

Magel2 null mice have increased adiposity and correspondingly higher circulating leptin levels (9). Progressive decline in leptin sensitivity through decreased LepR surface trafficking in POMC neurons has been suggested to be a contributing factor for the observed metabolic phenotypes (14–16). Consequently, impaired leptin → POMC neuron signaling would be predicted to cause reduced POMC neuron activity, and therefore hypoactivation of downstream MC4R expressing neurons. Here, we showed that POMC neuron firing properties are significantly altered (Fig. 2C and F). We observed that wild-type mice tend to have shorter inter-spike intervals between spikes compared with *Magel2*-null littermates in POMC neurons. Physiological significance of 'clustered' versus 'sparse' spike distribution is not clear; however, a recent report on *in vivo* activity of putative POMC neurons showed that shorter inter-event intervals are more common during morning hours, when animals are sated, compared with late afternoon when it is closer to feeding time (21). Release probability of large dense core vesicles, like those containing α-MSH, increases with spike frequency and this is believed to be owing to calcium accumulation in the axon terminals at higher firing rates (i.e. action potentials arriving in short intervals) (22). Future research will be required to see whether a switch from closely spaced events to longer intervals in *Magel2*-null mice may cause inefficient α-MSH release.

Interestingly, even if POMC neurons could be directly activated, they seem to have partially lost the ability to stimulate downstream neurons to promote satiety. It is notable that the reduced activation of POMC-dependent satiety pathways occurs despite the reported increase in sensitivity to MC4R agonists in these mice (14,17), suggesting that the downstream circuits are intact and indeed hyper-responsive to α-MSH release. It is also unlikely that other POMC neuron activated pathways, such as fast neurotransmitter release, might be impaired in *Magel2*-null mice. This is because lack of *Pomc* gene or complete ablation of POMC neurons causes similar phenotypes with respect to energy homeostasis, suggesting that POMC gene products constitute the key signaling agents in POMC neurons (23,24).

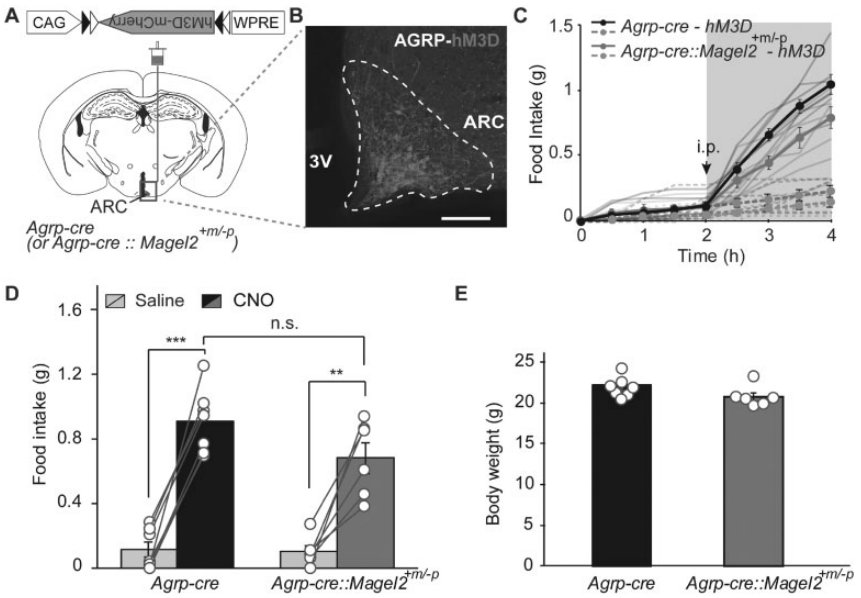

Figure 3. Appetite stimulating function of AGRP neurons is normal in *Magel2*-deficient mice. (**A**) Schematic representation for Cre-dependent rAAV expression of hM3D-mCherry in ARC^{AGRP} neurons. (**B**) Photomicrograph of hM3D-mCherry labeled AGRP neurons in arcuate nucleus. Scale: 100 μm. (**C**) Food intake graph before and after transient activation of AGRP neurons in *Agrp-cre* and littermate *Agrp-cre::Magel2*$^{+m/-p}$ mice by intraperitoneal saline (dashed line) or CNO administration (solid lines). (**D**) Summary graph for total food intake 2 h after saline or CNO administration (Saline-*Agrp-cre*: 0.11 ± 0.04 g, $n = 7$ and *Agrp-cre::Magel2*$^{+m/-p:}$ 0.10 ± 0.037 g, $n = 6$; $P = 0.86$; CNO-*Agrp-cre*: 0.92 ± 0.076 g, $n = 7$ and *Agrp-cre::Magel2*$^{+m/-p:}$ 0.69 ± 0.096 g, $n = 6$; $P = 0.087$). (**E**) Body weight graph for *Agrp-cre* and *Agrp-cre::Magel2*$^{+m/-p}$ mice (*Agrp-cre*: 21.76 ± 0.047 g, $n = 7$ and *Agrp-cre::Magel2*$^{+m/-p:}$ 20.69 ± 0.051 g, $n = 6$; $P = 0.16$).

Downloaded from https://academic.oup.com/hmg/article-abstract/27/18/3129/5033383 by guest on 08 January 2020

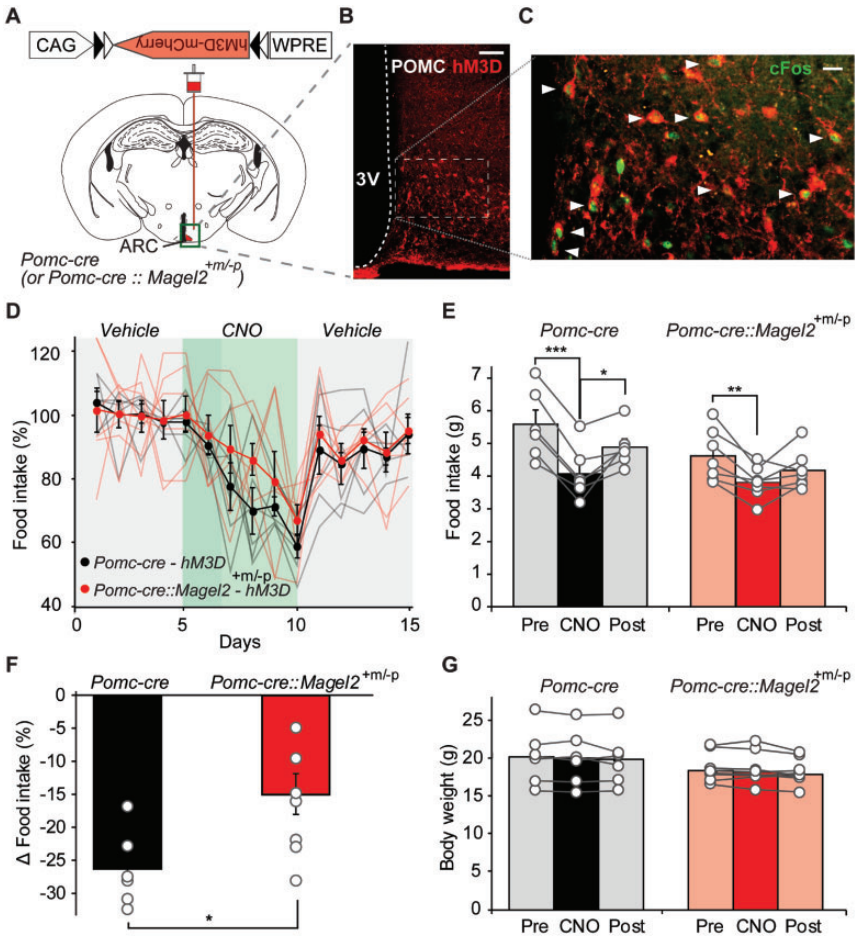

Figure 4. POMC neuron activity dependent loss of appetite is diminished in *Magel2*-null mice. (**A**) Schematic representation for Cre-dependent rAAV expression of hM3D-mCherry in ARC POMC neurons. (**B**) Photomicrograph of hM3D-mCherry labeled POMC neurons in arcuate nucleus. Scale: 100 μm. (**C**) Magnified images of CNO dependent cFos expression in *Pomc-cre::Magel2*$^{+m/-p}$ mouse expressing hM3Dq-mCherry. Scale: 30 μm. (**D**) Altered food intake resulted from chronic activation of POMC neurons in *Pomc-cre* and *Pomc-cre::Magel2*$^{+m/-p}$ mice by daily intraperitoneal CNO administration. (**E**) Summary graph for 5 days average food intake before, during and after intraperitoneal CNO injection (*Pomc-cre*: Pre −5.54 ± 0.08 g, CNO −4.07 ± 0.30 g, Post −4.85 ± 0.08 g, $n = 6$; Pre versus CNO $P = 0.0003$, CNO versus Post $P = 0.018$ and *Pomc-cre::Magel2*$^{+m/p}$: Pre −4.59 ± 0.02 g, CNO −3.78 ± 0.21 g, Post −4.15 ± 0.08 g, $n = 7$; Pre versus CNO $P = 0.004$, CNO versus Post $P = 0.109$). (**F**) Difference in POMC neuron-dependent suppression of food intake in *Pomc-cre* and *Pomc-cre::Magel2*$^{+m/p}$ mice (*Pomc-cre*: −26.35 ± 2.33%, $n = 6$ and *Pomc-cre::Magel2*$^{+m/-p}$: −14.96 ± 3.05%, $n = 7$; $P = 0.034$). (**G**) Body weight graph for *Pomc-cre* (Pre −20.23 ± 0.094 g, CNO −20.08 ± 0.172 g, Post −19.84 ± 0.014 g, $n = 6$) and *Pomc-cre::Magel2*$^{+m/-p}$ mice (Pre −18.33 ± 0.066 g, CNO −18.19 ± 0.093 g, Post −17.92 ± 0.043 g, $n = 7$) (*$P < 0.05$; **$P < 0.01$; ***$P < 0.001$).

Similarly, differential feeding response owing to selective sensitivity of *Magel2*-null mice to stress (25) is also unlikely to account for the observed impairment of POMC-induced satiety, since we did not detect any significant difference in feeding pattern in response to single housing or repeated i.p. injections between wild-type and *Magel2*-null animals (data not shown).

If the downstream circuits are intact (even sensitized), what then underlies the defective POMC neuron dependent satiety phenotype? Defects in cellular mechanisms responsible for synthesis, packaging or release of α-MSH are among possible candidates. Unlike other PWS mouse models (26,27), *Magel2*-null mice have been shown to contain decreased total number of ARC^{POMC} neurons likely owing to reduced somatic α-MSH synthesis (14). One implication of this would be decreased number of α-MSH containing terminals in projection target regions as well. Accordingly, two recent reports have shown 2- to 3-fold reductions in α-MSH labeling in paraventricular hypothalamic nucleus, one of the main POMC downstream targets (11,15). It should be noted that, in addition to POMC neuron loss, impaired axonal growth may also contribute to the reported reduction in α-MSH containing boutons. Such a noteworthy decline in α-MSH release sites is consistent with our observations that even with extensive chemogenetic activation and hyperresponsive downstream MC4R signaling machinery, POMC neurons fail to effectively suppress appetite in *Magel2* deficient background.

Voracious food seeking and consumption seen in PWS patients are reminiscent of acute AGRP neuron activation phenotype seen in mice (19,28); however, deleting *Magel2* alone is not sufficient to recapitulate this behavior. Our results showed that, unlike POMC circuits, AGRP neuron activity levels and its ability to adapt energy needs appeared to be normal in *Magel2* null mice (Fig. 1). Furthermore, feeding that is typically observed with AGRP neuron activation is indistinguishable between wild-type and *Magel2* deficient animals (Fig. 3), suggesting that there is no additional sensitization in AGRP neuron circuits. Earlier works have shown higher circulating ghrelin levels in human subjects with PWS (29), leading to the suggestion that its hypothalamic orexigenic targets, such as AGRP neurons, might be over activated. Similar

Downloaded from https://academic.oup.com/hmg/article-abstract/27/18/3129/5033383 by guest on 08 January 2020

changes in ghrelin levels have been reported for a PWS mouse model with larger regional deletion (30) but *Magel2*-null mice appears to have normal active plasma ghrelin levels and normal ghrelin response (11). Consistently, we did not observe significant difference in ghrelin induced feeding in *Magel2*-null mice. It is important to note that we only monitored short term appetite related impact of i.p. administered ghrelin, and we cannot rule out possible defects in other ghrelin related functions. Indeed, there is evidence for impaired growth hormone release and IGF1 function in MAGEL2 deficiency (25,31). Our work with AGRP neurons suggest that MAGEL2 protein is not essential for normal AGRP neuron evoked appetite nor its absence makes AGRP neuron dependent feeding any more forceful.

Unlike AGRP neurons, POMC neurons have limited impact on short-term regulation of appetite (20,28,32). Nevertheless, defective POMC neuron activation phenotype in *Magel2* null mice described here would help explain several aspects of PWS, including increased fat mass, reduced activity and infertility. Since some of the previously described *Magel2* deficiency phenotypes were sex-specific, future research will be required to see if impaired POMC-satiety pathway extends to female mice. Collectively, our results demonstrate that *Magel2* deficient mice have selective loss of function in POMC but not in AGRP neuron circuits. Our results corroborate earlier reports about LepR dysfunction in POMC neurons and provide insight into functional implications of *Magel2* deficiency by showing that MAGEL2 is required for both normal activity patterns as well as effective subsequent α-MSH release for MC4R activation.

Materials and Methods

Animals

All animal care, maintenance, husbandry and experimental procedures were approved by Istanbul Medipol University Animal Care and Use Committee. Animals were housed at 22–24°C on a 12-h light (06:00) and dark (18:00) cycle. C57BL/6-*Magel2*^{tm1Stw}/J (Jackson Labs Stock 009062), *Agrp*$^{tm1(cre)Lowl}$/J (Jackson Labs Stock 012899) and Pomc-cre$^{1Lowl/J}$ (Jackson Labs Stock 010714) lines were used. All lines were maintained through mating with C57BL/6 background. To generate *Magel2*-null *Agrp-cre* and *Pomc-cre* mice, females from these Cre-expressing driver lines were crossed to male mice carrying *Magel2*-null copy, *Agrp-cre* and *Pomc-cre* controls are chosen from littermates. Mice were given *ad libitum* access to water and standard mouse chow unless noted otherwise. For electrophysiology, male and female mice were used, while for behavioral experiments only 8–10 weeks old male mice were used.

Stereotaxic rAAV injections

Virus injections were performed as described previously (19). Briefly, mice were anaesthetized with isoflurane using stereotaxic instrument (David Kopf instruments, Tujunga, CA, USA) and scalp was incised carefully before drilling the skull for injection. Two hundred and fifty to three hundred nanoliters of intracranial injection were performed with a pulled glass pipette (Drummond Scientific, Wiretrol, Broomall, PA, USA) having 40–50 μm tip diameter. Recombinant adeno-associated virus production was conducted as described previously (33). Cre-dependent AAV vectors *rAAV2/1-EF1a-DIO-hM3D(Gq)-mCherry* and *rAAV2/8-FLEX-GFP* were purchased from Addgene http://www.addgene.org/. *rAAV2/1-EF1a-DIO-hM3D(Gq)-mCherry* (2×10^{12} genomic copies/ml) or *rAAV2/8-FLEX-GFP* (10^{14} genomic copies/ml) was injected at coordinates around the ARC (bregma: −1.25 mm, midline: ±0.25 mm, dorsal surface −5.20 and −5.70 mm). Injection speed was set to 30 nl/min by a micromanipulator (Narishige, East Meadow, NY, USA). Following first intracranial injection at −5.70 mm dorsal surface, another intracranial injection was performed at −5.20 mm dorsal surface, allowing 10 min time for each injection. Injection pipette was slowly withdrawn and the scalp was stitched. Animals were allowed 14 days for recovery and transgene expression.

Electrophysiology

All *ex vivo* recordings were done as previously described (19). Briefly, P45-P50 mice were used for viral infection, after 10–14 days, mice were deeply anaesthetized with isoflurane and decapitated. All slice preparations were performed in early morning hours, unless noted otherwise. The brain was removed and placed in an ice-cold cutting solution containing (in mM): 234 sucrose, 28 $NaHCO_3$, 7 dextrose, 2.5 KCl, 7 $MgCl_2$, 0.5 $CaCl_2$, 1 sodium ascorbate, 3 sodium pyruvate and 1.25 NaH_2PO_4, aerated with 95% O_2/5% CO_2. Three hundred micrometers thick coronal slices containing the arcuate nucleus were sectioned using vibratome (Leica VT1000S) and transferred to artificial cerebrospinal fluid (aCSF) containing (in mM): 119 NaCl, 25 $NaHCO_3$, 11 D-glucose, 2.5 KCl, 1.25 $MgCl_2$, 2 $CaCl_2$ and 1.25 NaH_2PO_4, aerated with 95% O_2/5% CO_2. Before the recordings, slices were incubated in oxygenated aCSF for 30 min at room temperature and recorded at same conditions (20–24°C). The cells were identified and targeted by green fluorescence emission. Neurons were patched using electrodes with 4–5 MΩ tip resistances. An aCSF was used for the intracellular solution during cell-attached recordings.

Food intake analysis

Following two weeks post-operative recovery time, to record food intake of individual animals, mice were single housed for 2 days prior to the feeding analysis to acclimatize to feeding cages and minimize isolation stress. Also animals were handled for a week to minimize handling stress during i.p. injections. *Agrp-cre*, *Agrp-cre*::*Magel2*$^{+m/-p}$, *Pomc-cre* and *Pomc-cre*::*Magel2*$^{+m/-p}$ mice were injected with hM3D(Gq)-mCherry and fed *ad libitum* for food intake studies. In the light cycle, food consumption of *Agrp-cre* and *Agrp-cre*::*Magel2*$^{+m/-p}$ mice were monitored for 2 h for baseline. Ghrelin is obtained from Bachem. A 2 mg/kg CNO (Tocris) or saline was administered intraperitoneally and food intake was measured for two more hours. For *Pomc-cre* and *Pomc-cre*::*Magel2*$^{+m/-p}$ mice, chronic chemogenetic manipulations were performed. Mice transduced with *hM3D(Gq)-mCherry* were treated with saline, CNO (2 mg/kg) and saline subsequently (and prior to CNO as well), for three times a day with 8 h intervals, 5 days each. Food consumptions and body weights were recorded.

Immunohistochemistry and imaging

Animals were transcardially perfused with 4% paraformaldehyde in 0.1 M pH 7.4 phosphate buffer fixative. Brains were collected and post-fixed with the same solution for 4 h, 75 μm brain sections were obtained with vibratome and washed in 0.1 M phosphate-buffered saline with Triton X-100 (PBST). Brain sections were blocked in 5% normal goat serum/PBST for 1 h in room temperature and overnight incubation was performed at

Downloaded from https://academic.oup.com/hmg/article-abstract/27/18/3129/5033383 by guest on 08 January 2020

+4°C in blocking solution containing the primary antibody (anti-cFos, 1:5000, Cell Signaling). Slices were then rinsed with PBST, incubated with secondary antibody [goat anti-rabbit IgG (H + L) Alexa Flour 488, 1:500, Invitrogen] for 1 h in room temperature and washed with PBST again. Brain sections were transferred to microscope slides and mounted with Fluoromount (Sigma F4680) for imaging. Brain images were obtained by confocal microscopy (Carl Zeiss, Thornwood, NY, USA).

Statistical analysis

All data were presented as means ± SEM. Student's *t*-test was used to analyze significance of firing frequency and cumulative food intake between *Agrp-cre* and *Agrp-cre::Magel2*$^{+m/-p}$, as well as *Pomc-cre and Pomc-cre::Magel2*$^{+m/-p}$.

Supplementary Material

Supplementary Material is available at *HMG* online.

Conflict of Interest statement. None declared.

Funding

This work was supported by European Molecular Biology Organisation (EMBO) Installation Grant to D.A., grant no. 2539.

References

1. Burnside, R.D., Pasion, R., Mikhail, F.M., Carroll, A.J., Robin, N.H., Youngs, E.L., Gadi, I.K., Keitges, E., Jaswaney, V.L., Papenhausen, P.R. *et al.* (2011) Microdeletion/microduplication of proximal 15q11.2 between BP1 and BP2: a susceptibility region for neurological dysfunction including developmental and language delay. *Hum. Genet.*, **130**, 517–528.
2. Dykens, E.M. and Kasari, C. (1997) Maladaptive behavior in children with Prader–Willi syndrome, Down syndrome, and nonspecific mental retardation. *Am. J. Ment. Retard.*, **102**, 228–237.
3. Holm, V.A., Cassidy, S.B., Butler, M.G., Hanchett, J.M., Greenswag, L.R., Whitman, B.Y. and Greenberg, F. (1993) Prader–Willi syndrome: consensus diagnostic criteria. *Pediatrics*, **91**, 398–402.
4. Milner, K.M., Craig, E.E., Thompson, R.J., Veltman, M.W., Thomas, N.S., Roberts, S., Bellamy, M., Curran, S.R., Sporikou, C.M. and Bolton, P.F. (2005) Prader–Willi syndrome: intellectual abilities and behavioural features by genetic subtype. *J. Child Psychol. Psychiatry*, **46**, 1089–1096.
5. Bittel, D.C. and Butler, M.G. (2005) Prader–Willi syndrome: clinical genetics, cytogenetics and molecular biology. *Expert Rev. Mol. Med.*, **7**, 1–20.
6. Hanel, M.L. and Wevrick, R. (2001) The role of genomic imprinting in human developmental disorders: lessons from Prader–Willi syndrome. *Clin. Genet.*, **59**, 156–164.
7. Schaaf, C.P., Gonzalez-Garay, M.L., Xia, F., Potocki, L., Gripp, K.W., Zhang, B., Peters, B.A., McElwain, M.A., Drmanac, R., Beaudet, A.L. *et al.* (2013) Truncating mutations of MAGEL2 cause Prader–Willi phenotypes and autism. *Nat. Genet.*, **45**, 1405–1408.
8. Fountain, M.D., Jr. and Schaaf, C.P. (2015) MAGEL2 and oxytocin-implications in Prader–Willi syndrome and beyond. *Biol. Psychiatry*, **78**, 78–80.
9. Bischof, J.M., Stewart, C.L. and Wevrick, R. (2007) Inactivation of the mouse Magel2 gene results in growth abnormalities similar to Prader–Willi syndrome. *Hum. Mol. Genet.*, **16**, 2713–2719.
10. Kozlov, S.V., Bogenpohl, J.W., Howell, M.P., Wevrick, R., Panda, S., Hogenesch, J.B., Muglia, L.J., Van Gelder, R.N., Herzog, E.D. and Stewart, C.L. (2007) The imprinted gene Magel2 regulates normal circadian output. *Nat. Genet.*, **39**, 1266–1272.
11. Maillard, J., Park, S., Croizier, S., Vanacker, C., Cook, J.H., Prevot, V., Tauber, M. and Bouret, S.G. (2016) Loss of Magel2 impairs the development of hypothalamic anorexigenic circuits. *Hum. Mol. Genet.*, **25**, 3208–3215.
12. Sternson, S.M. and Atasoy, D. (2014) Agouti-related protein neuron circuits that regulate appetite. *Neuroendocrinology*, **100**, 95–102.
13. Henry, F.E., Sugino, K., Tozer, A., Branco, T. and Sternson, S.M. (2015) Cell type-specific transcriptomics of hypothalamic energy-sensing neuron responses to weight-loss. *Elife*, **4**,
14. Mercer, R.E., Michaelson, S.D., Chee, M.J., Atallah, T.A., Wevrick, R. and Colmers, W.F. (2013) Magel2 is required for leptin-mediated depolarization of POMC neurons in the hypothalamic arcuate nucleus in mice. *PLoS Genet.*, **9**, e1003207.
15. Pravdivyi, I., Ballanyi, K., Colmers, W.F. and Wevrick, R. (2015) Progressive postnatal decline in leptin sensitivity of arcuate hypothalamic neurons in the Magel2-null mouse model of Prader–Willi syndrome. *Hum. Mol. Genet.*, **24**, 4276–4283.
16. Wijesuriya, T.M., De Ceuninck, L., Masschaele, D., Sanderson, M.R., Carias, K.V., Tavernier, J. and Wevrick, R. (2017) The Prader–Willi syndrome proteins MAGEL2 and necdin regulate leptin receptor cell surface abundance through ubiquitination pathways. *Hum. Mol. Genet.*, **26**, 4215–4230.
17. Bischof, J.M., Van Der Ploeg, L.H., Colmers, W.F. and Wevrick, R. (2016) Magel2-null mice are hyper-responsive to setmelanotide, a melanocortin 4 receptor agonist. *Br. J. Pharmacol.*, **173**, 2614–2621.
18. Wang, Q., Liu, C., Uchida, A., Chuang, J.C., Walker, A., Liu, T., Osborne-Lawrence, S., Mason, B.L., Mosher, C., Berglund, E.D. *et al.* (2014) Arcuate AgRP neurons mediate orexigenic and glucoregulatory actions of ghrelin. *Mol. Metab.*, **3**, 64–72.
19. Atasoy, D., Betley, J.N., Su, H.H. and Sternson, S.M. (2012) Deconstruction of a neural circuit for hunger. *Nature*, **488**, 172–177.
20. Zhan, C., Zhou, J., Feng, Q., Zhang, J.E., Lin, S., Bao, J., Wu, P. and Luo, M. (2013) Acute and long-term suppression of feeding behavior by POMC neurons in the brainstem and hypothalamus, respectively. *J. Neurosci.*, **33**, 3624–3632.
21. Mandelblat-Cerf, Y., Ramesh, R.N., Burgess, C.R., Patella, P., Yang, Z., Lowell, B.B. and Andermann, M.L. (2015) Arcuate hypothalamic AgRP and putative POMC neurons show opposite changes in spiking across multiple timescales. *eLife*, **4**, 1–25.
22. van den Pol, A.N. (2012) Neuropeptide transmission in brain circuits. *Neuron*, **76**, 98–115.
23. Yaswen, L., Diehl, N., Brennan, M.B. and Hochgeschwender, U. (1999) Obesity in the mouse model of pro-opiomelanocortin deficiency responds to peripheral melanocortin. *Nat. Med.*, **5**, 1066–1070.
24. Gropp, E., Shanabrough, M., Borok, E., Xu, A.W., Janoschek, R., Buch, T., Plum, L., Balthasar, N., Hampel, B., Waisman, A. *et al.* (2005) Agouti-related peptide-expressing neurons are mandatory for feeding. *Nat. Neurosci.*, **8**, 1289–1291.
25. Tennese, A.A. and Wevrick, R. (2011) Impaired hypothalamic regulation of endocrine function and delayed

Downloaded from https://academic.oup.com/hmg/article-abstract/27/18/3129/5033383 by guest on 08 January 2020

counterregulatory response to hypoglycemia in Magel2-null mice. *Endocrinology*, **152**, 967–978.
26. Qi, Y., Purtell, L., Fu, M., Lee, N.J., Aepler, J., Zhang, L., Loh, K., Enriquez, R.F., Baldock, P.A., Zolotukhin, S. *et al.* (2016) Snord116 is critical in the regulation of food intake and body weight. *Sci. Rep.*, **6**, 18614.
27. Ge, Y., Ohta, T., Driscoll, D.J., Nicholls, R.D. and Kalra, S.P. (2002) Anorexigenic melanocortin signaling in the hypothalamus is augmented in association with failure-to-thrive in a transgenic mouse model for Prader–Willi syndrome. *Brain Res.*, **957**, 42–45.
28. Aponte, Y., Atasoy, D. and Sternson, S.M. (2011) AGRP neurons are sufficient to orchestrate feeding behavior rapidly and without training. *Nat. Neurosci.*, **14**, 351–355.
29. DelParigi, A., Tschop, M., Heiman, M.L., Salbe, A.D., Vozarova, B., Sell, S.M., Bunt, J.C. and Tataranni, P.A. (2002) High circulating ghrelin: a potential cause for hyperphagia and obesity in Prader–Willi syndrome. *J. Clin. Endocrinol. Metab.*, **87**, 5461–5464.
30. Stefan, M., Ji, H., Simmons, R.A., Cummings, D.E., Ahima, R.S., Friedman, M.I. and Nicholls, R.D. (2005) Hormonal and metabolic defects in a Prader–Willi syndrome mouse model with neonatal failure to thrive. *Endocrinology*, **146**, 4377–4385.
31. McCarthy, J.M., McCann-Crosby, B.M., Rech, M.E., Yin, J., Chen, C.A., Ali, M.A., Nguyen, H.N., Miller, J.L. and Schaaf, C.P. (2018) Hormonal, metabolic and skeletal phenotype of Schaaf-Yang syndrome: a comparison to Prader–Willi syndrome. *J. Med. Genet.*, **55**, 307–315.
32. Fenselau, H., Campbell, J.N., Verstegen, A.M., Madara, J.C., Xu, J., Shah, B.P., Resch, J.M., Yang, Z., Mandelblat-Cerf, Y., Livneh, Y. *et al.* (2017) A rapidly acting glutamatergic ARC–>PVH satiety circuit postsynaptically regulated by alpha-MSH. *Nat. Neurosci.*, **20**, 42–51.
33. Mathews, L.C., Gray, J.T., Gallagher, M.R. and Snyder, R.O. (2002) Recombinant adeno-associated viral vector production using stable packaging and producer cell lines. *Methods Enzymol.*, **346**, 393–413.

Downloaded from https://academic.oup.com/hmg/article-abstract/27/18/3129/5033383 by guest on 08 January 2020